Author Accepted Manuscript version of the paper by Lisa Reis et al.
in 2023 IEEE PES Innovative Smart Grid Technologies Conference Europe - ISGT-Europe (2023),
https://doi.org/10.1109/ISGTEUROPE56780.2023.10407790

Polynomial Fitting of Operating Point Dependency in Small-Signal State-Space Models for Power Electronic Converters

[*,#]Lisa Reis
[*]*Dept. of Electrical and Computer Eng.*
RPTU Kaiserslautern-Landau
Kaiserslautern, Germany
reis@eit.uni-kl.de

[§]Andrew Macmillan Smith,
[§]Salvatore D'Arco
[§]*SINTEF Energy Research*
Trondheim, Norway
{andrew.smith, salvatore.darco}@sintef.no

[§,#]Jon Are Suul
[#]*Dept. of Engineering Cybernetics*
NTNU
Trondheim, Norway
jon.are.suul@ntnu.no

***Abstract*—This paper presents an approach for representing nonlinear operating point dependencies in small-signal state-space modelling of power electronic converters. The intended application is for unifying a set of small-signal models identified from black-box simulation models or physical measurements into a single operating point dependent model. The approach is based on a polynomial fitting of the operating point dependency of the matrix elements in a state-space modal representation. The fitted expressions for the matrix elements provide a single model that can be utilized for small-signal analysis in a wide range of operating conditions and prevents the need for investigation of individual models at each operation point. Two different cases are discussed for evaluating the applicability of the presented approach, including a grid-forming converter with a Virtual Synchronous Machine (VSM)-based control and a conventional grid-following converter with dc-link voltage control. The results show that a quadratic fitting of the matrix elements can provide acceptable model accuracy in most cases.**

***Index Terms*—power electronic systems, model identification, state-space models, small-signal analysis, MIMO-systems, laboratory experiments**

I. Introduction

Eigenvalue-based analysis provides an established framework for assessing small-signal stability in power systems [1], [2] and is currently being adapted to the emerging conditions with dominant presence of power electronic converters [3], [4]. The calculation of eigenvalues relies on a linearized state-space model of the studied system. When a sub-system model is not directly available, it must be identified, either from a black-box model or from measurements on a physical unit [5], [6]. Since power converters have inherent nonlinear characteristics, the linearized state-space models will depend on the operating conditions. Thus, state-space models must be identified for all the operating conditions to be considered. For screening of stability characteristics over a wide range of operating conditions, this will require a high number of models as an individual model must be defined for each operating point to be considered. Furthermore, for analysis relying on model identification from measurements, all operating points to be considered must be defined in advance to obtain the required data-sets. Therefore, a simple way to express the operating point dependency of state-space models continuously throughout the operating range could be useful to support small-signal analysis of systems including black-box models.

Several examples of parameterized macromodeling approaches have been proposed to handle variations in operating conditions for state-space models. For instance, a multivariate orthonormal vector fitting was developed in [7] to represent frequency-dependency as well as parameter-dependencies in fitted models. Similar methods are used in [8], [9], [10] to develop geometry- or material parameter-dependent models. In particular, [9] presents an example of a small-signal analysis that is quite reminiscent of an analysis performed for power electronic converters. If input conditions are treated as parameters, the parameterized macromodeling techniques can be applied to the context of operating point dependency. This is addressed in [11] by creating bias point-dependent linear models for small-signal power integrity analyses.

This paper proposes a state-space modelling approach where the dependency on operating conditions is fitted into the expressions of the matrix elements. Thus, for each matrix element a polynomial expression is fitted as a function of the inputs. This allows for generating the linearized state space model of the power converter at any operating point without the need for an individual model identified with the specific combination of input signals. For example, the eigenvalue trajectories can be obtained as a function of the input signals with any resolution, equivalently to an interpolation between the points used for fitting of the matrix elements.

The introduced methodology for fitting the operating point dependency into the matrix elements is a novel approach for small-signal modelling and analysis, developed from [12], and this paper presents a first application to the modelling of power electronic converters. In the presented implementation, the operation point dependency of the matrix elements is approximated by superposition of the influence from each

The work was supported by the Ocean Grid Research Project, funded by the Green Platform instrument of the Research Council of Norway under Grant 328750.

Author Accepted Manuscript version of the paper by Lisa Reis et al.
in 2023 IEEE PES Innovative Smart Grid Technologies Conference Europe - ISGT-Europe (2023),
https://doi.org/10.1109/ISGTEUROPE56780.2023.10407790

input. To ensure a clear reference for performance assessment, the development and verification of the approach is based on the analytical linearized state-space models of two cases for a voltage source converter (VSC) with different control systems. The first example is a virtual synchronous machine (VSM) as documented in [13], while the second example is a grid-following converter with dc voltage control (VDC) as documented in [14]. The results from these two cases highlight the potential performance and advantages of the proposed modelling approach. The results also reveal the limitations that appear for systems where the nature of the small-signal dynamics change significantly with the operating conditions.

II. Polynomial Fitting of Operating Point Dependency

Small-signal analysis of dynamic systems can be conducted with a state-space model linearized at a steady state operating point. The general linearized state-space formulation is given by (1) and relates the variations in the states $\mathbf{\Delta x}$ and in the output $\mathbf{\Delta y}$ to the inputs $\mathbf{\Delta u}$ via the matrices $\mathbf{A}$, $\mathbf{B}$, $\mathbf{C}$ and $\mathbf{D}$. These matrices are in general a function of the linearization point defined by $(\mathbf{x}_0, \mathbf{u}_0)$.

$$\begin{aligned} \Delta\dot{\mathbf{x}} &= \mathbf{A}(\mathbf{x}_0, \mathbf{u}_0) \cdot \Delta\mathbf{x} + \mathbf{B}(\mathbf{x}_0, \mathbf{u}_0) \cdot \Delta\mathbf{u} \\ \Delta\mathbf{y} &= \mathbf{C}(\mathbf{x}_0, \mathbf{u}_0) \cdot \Delta\mathbf{x} + \mathbf{D}(\mathbf{x}_0, \mathbf{u}_0) \cdot \Delta\mathbf{u} \end{aligned} \tag{1}$$

An equilibrium point of a nonlinear model corresponds to zero state derivatives and can be found by solving a system of algebraic equations as a function of the input signal. Thus, the steady state operating point defined by $\mathbf{x}_0$ is linked to the input conditions $\mathbf{u}_0$ via a nonlinear function that generally cannot be computed in closed form:

$$\mathbf{x}_0 = \mathbf{g}(\mathbf{u_0}) \tag{2}$$

Thus, the linearized state space form can be rewritten to explicitly indicate the dependence on the operating point as:

$$\begin{aligned} \Delta\dot{\mathbf{x}} &= \mathbf{A}(\mathbf{g}(\mathbf{u_0}), \mathbf{u}_0) \cdot \Delta\mathbf{x} + \mathbf{B}(\mathbf{g}(\mathbf{u_0}), \mathbf{u}_0) \cdot \Delta\mathbf{u} \\ \Delta\mathbf{y} &= \mathbf{C}(\mathbf{g}(\mathbf{u_0}), \mathbf{u}_0) \cdot \Delta\mathbf{x} + \mathbf{D}(\mathbf{g}(\mathbf{u_0}), \mathbf{u}_0) \cdot \Delta\mathbf{u} \end{aligned} \tag{3}$$

Within a certain range of operating conditions, it is assumed that the functional dependency of the state space matrices on the operating conditions can be approximated with a simpler form and, in the specific case of this paper, with a polynomial function.

$$\begin{aligned} \mathbf{A}(\mathbf{g}(\mathbf{u_0}), \mathbf{u}_0) &\approx \tilde{\mathbf{A}}(\mathbf{u_0}) \\ \mathbf{B}(\mathbf{g}(\mathbf{u_0}), \mathbf{u}_0) &\approx \tilde{\mathbf{B}}(\mathbf{u_0}) \\ \mathbf{C}(\mathbf{g}(\mathbf{u_0}), \mathbf{u}_0) &\approx \tilde{\mathbf{C}}(\mathbf{u_0}) \\ \mathbf{D}(\mathbf{g}(\mathbf{u_0}), \mathbf{u}_0) &\approx \tilde{\mathbf{D}}(\mathbf{u_0}) \end{aligned} \tag{4}$$

With this assumption, each element of the state matrices is approximated by a polynomial expression of the inputs. For example, if $a_{i,j}$ is a generic element of $\mathbf{A}$, the objective is to identify a polynomial expression $f_{a_{i,j}}(\mathbf{u_0})$ such that (5) applies.

$$a_{i,j}(\mathbf{u_0}) \approx \tilde{a}_{i,j}(\mathbf{u_0}) = f_{a_{i,j}}(\mathbf{u_0}) \tag{5}$$

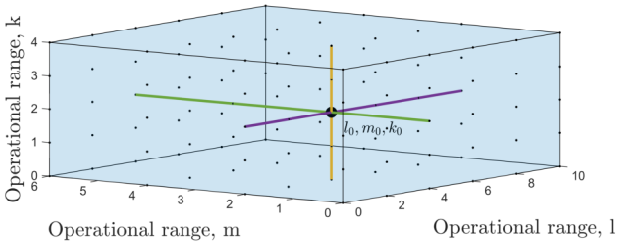

Fig. 1: Example sweeps for a three-input system

A state space representation is not unique since it depends on the particular choice of the states. Indeed, infinite equivalent state-state representations can be obtained by similarity transformations. To create a fit, it is crucial that the representation of the system is consistent when varying the operating conditions. In this paper a modal representation is preferred. Thus, the matrix $\mathbf{A}$ is a block diagonal matrix, where the blocks represent the eigenvalues. To obtain a consistent representation, further conventions concerning the state order and the scaling of the B and C matrix are also needed, as discussed in [12]. A main advantage of the modal representation is that each state can directly be associated with an eigenvalue, which is useful to maintain a consistent order of states. For the application of the method to a set of identified state-space systems, this also enables easy filtering of identification errors and outliers.

III. Fitting Process and Superposition

The proposed fitting process provides a polynomial approximation of the elements of the state matrices to incorporate the dependencies on the operating condition. While the intended application is for small-signal models that are identified from a black-box model, a complete nonlinear state-space model is used in the following as the starting point for analysis. As a first step, the domain of the operating conditions is discretized by dividing the range of variability for each input into a finite number of values. This is illustrated in Fig. 1, assuming three inputs (i.e. k, l, m) where each node corresponds to a considered operating condition. For each operating point in this discretized domain, the system can be linearized and the four state matrices calculated. Considering the three inputs from Fig. 1, three additional indexes can be added to represent the matrix element for a specific input combination leading to $a_{i,j,k,l,m}$, $b_{i,j,k,l,m}$, $c_{i,j,k,l,m}$, and $d_{i,j,k,l,m}$. The indexes i and j represent the position of the element in the matrix while the indexes k, l, m represent the input values. The objective is to identify a polynomial function for each matrix element, representing the dependency of the matrix element from the input values.

$$a_{i,j,k,l,m} \approx f_{a_{i,j}}(k, l, m) \tag{6}$$

Although possible, fitting functions with multiple independent variables requires a large number of data points, where, in practice, the acquisition of each data point is connected to high computational effort. Also, the number of input value combinations increases exponentially with the number of input values. Therefore, for systems with multiple inputs, there is a

Author Accepted Manuscript version of the paper by Lisa Reis et al.
in 2023 IEEE PES Innovative Smart Grid Technologies Conference Europe - ISGT-Europe (2023),
https://doi.org/10.1109/ISGTEUROPE56780.2023.10407790

TABLE I: Input ranges in p.u.

Input VSM	Range (Def.)	Input Vdc	Range (Def.)
active power ref. p^*	0-1 (0.5)	q-current ref. $i_{\mathrm{l,q}*}$	-0.5-0.5 (0)
reactive power ref. q^*	-1-1 (0)	grid voltage v_{g}	0.9-1.1 (1)
grid voltage v_{g}	0.9-1.1 (1)	grid freq. ω_{g}	0.95-1.04 (1)
voltage ref. v^*	0.9-1.1 (1)	dc-current $i_{\mathrm{dc,s}}$	-1-1[a] (0.1)
grid freq. ω_{g}	0.95-1.04 (1)	dc-voltage ref. v^*_{dc}	0.9-1.1 (1)
frequency ref. ω^*	0.95-1.04 (1)		

[a] range was limited to 0.1 to 0.3 for the fitting to prevent pole bifurcation

need for further simplification. The proposed method is carried out as a two-step process.

In the first step, the dependency on each individual input is determined by sweeping each input variable separately over the input range while all other input variables maintain their default values. For example, for input k the deviation $f_{a_{i,j},k}$ of one matrix element $a_{i,j}$ from its value at the default operating point k_0 is assumed with a polynomial expression as:

$$f_{a_{i,j},k}(k-k_0) = p_{a_{i,j},k,1}(k-k_0) + p_{a_{i,j},k,2}(k-k_0)^2 + \ldots \tag{7}$$

where $p_{a_{i,j},k,1}$ and $p_{a_{i,j},k,2}$ are the coefficients determined in the fitting process. This first step covers the operating points on the sweep axes marked in Fig. 1. In the second step of the process, operating points with more than one input variable deviating from the default operating condition are approximated by superposition of the individual input dependencies from single-variable sweeps as:

$$\begin{aligned} f_{a_{i,j}}(k,l,m) = a_{i,j}(k_0,l_0,m_0) + f_{a_{i,j},k}(k-k_0) + \\ + f_{a_{i,j},l}(l-l_0) + f_{a_{i,j},m}(m-m_0) \end{aligned} \tag{8}$$

where k_0, l_0 and m_0 mark the default operating point where the individual variable sweeps intersect, and each of the functions $f_{a_{i,j},k}$, $f_{a_{i,j},l}$ and $f_{a_{i,j},m}$ describe the dependency on the corresponding input alone.

IV. Application of the Fitting Process

A. Example cases

The process described in the previous section has been applied to two power electronic converter configurations:

1) A grid-forming converter controlled as a Virtual Synchronous Machine (VSM) according to [13]. The model includes a virtual swing equation with active power-frequency droop, and voltage-reactive power droop, current reference calculation by a virtual impedance, current controllers and active damping. The dc side voltage is assumed to be constant. The system order and, respectively, the number of states is 18.
2) A grid-following converter with dc-voltage control (VDC), as used in [14]. The model includes the same current control and active damping as the VSM-case, a PLL for grid synchronization, and a PI-controller for regulating the dc-voltage by providing the d-axis current reference. This model also has 18 states.

Table I shows the inputs with corresponding sweep ranges and default values for each system. The outputs for both models are the d- and q-components of the filter inductor current, the output voltage and the output current. The VDC model has in addition the dc-voltage as output.

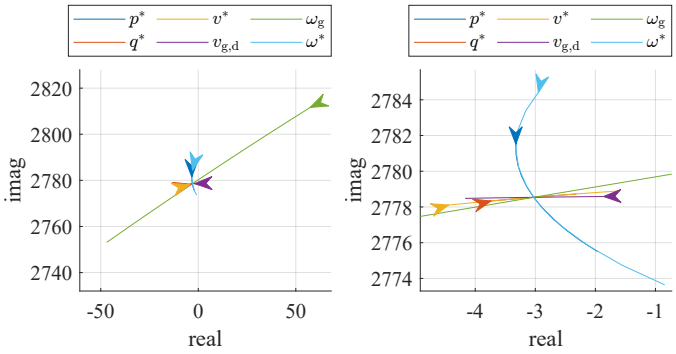

Fig. 2: Trajectories of one example eigenvalue of the VSM for all individual input sweeps total view (left) and zoomed in (right). The arrow marks the lower limit of the sweep.

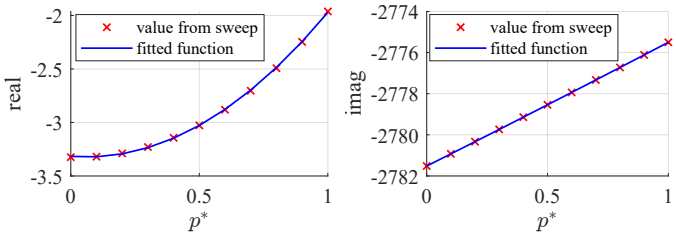

Fig. 3: Dependencies of real part (left) and imaginary part (right) of one example eigenvalue of the VSM for a sweep of p^*

B. Model Generation

The input ranges have been discretized with 11 points each as an initial step, and the resolution has been increased wherever necessary. Fig. 2 shows the trajectories of one example eigenvalue of the VSM for all input sweeps. This eigenvalue is the one with the highest influence on the input-output behaviour according to the Hankel singular value it can be associated with. The input ω_{g} has the highest impact on the system. The characteristic of the droop controllers can be seen since p^* and ω^* as well as q^* and v^* share a trajectory.

Fig. 3 shows the real and imaginary part of one example eigenvalue of the VSM for the sweep of p^*. It displays the values obtained from the sweep as well as the fitted functions. It can be seen that both dependencies can be described well by the chosen quadratic function.

While the approach proved successful for the VSM model as discussed for Fig. 3, the second model introduces major challenges to the presented approach. Firstly, the VSM model has eigenvalues that are either consistently real or consistently complex throughout the whole sweep, which means that there are no bifurcation points. For the second model, several eigenvalues reach bifurcation points if the sweep of $i_{\mathrm{dc,s}}$ spans from -1 to 1. Moreover, the eigenvalues are located in very close vicinity and their trajectories intersect. In this case, more steps throughout the sweep were needed to anticipate the trajectories over the whole input range. Fig. 4 displays

Author Accepted Manuscript version of the paper by Lisa Reis et al.
in 2023 IEEE PES Innovative Smart Grid Technologies Conference Europe - ISGT-Europe (2023),
https://doi.org/10.1109/ISGTEUROPE56780.2023.10407790

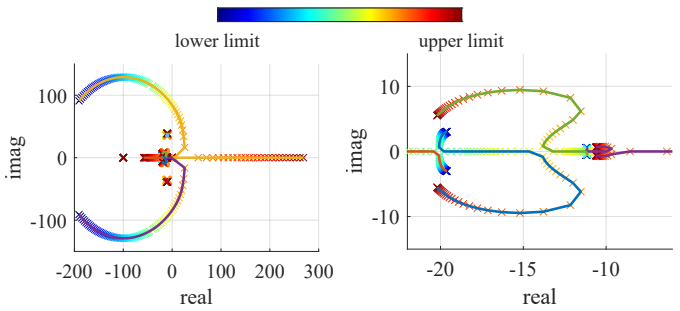

Fig. 4: Trajectories of the ten eigenvalues with the smallest real parts (left) and a zoomed view (right) for the VDC model with a sweep of $i_{\mathrm{dc,s}}$ from -1 to 1

this behaviour for a sweep with 101 values. For the following discussion, the input range of $i_{\mathrm{dc,s}}$ is limited to 0.1 to 0.3, so that no bifurcation points appear during the sweep and fitting without piecewise function definition is possible.

V. Validation of Results

The validation of the method is performed in two steps: first, by calculating the accuracy of the fitted model while varying a single variable at a time. An evenly spaced array between the upper and lower limit of the respective range for each input is examined, while the remaining inputs are held constant at the nominal operating point. The second part of the validation consists of varying two inputs simultaneously while holding the rest constant to examine the validity of the superposition approximation. A 2D grid is examined for each pair, although with a courser mesh than the single variable sweeps due to the exponential nature of possible operating points (31 points per input as opposed to 101).

The fitted model is compared to the analytical model at each operating point for each transfer function in the frequency domain by using the normalized root mean squared error (NRMSE), given as:

$$\mathrm{NRMSE}(\mathbf{H}, \mathbf{H}_0) = \left(1 - \frac{||\mathbf{H}_0 - \mathbf{H}||}{||\mathbf{H}_0 - \mathrm{mean}(\mathbf{H})||}\right) \cdot 100\% \quad (9)$$

where $\mathbf{H}_0$ is the reference data set for the frequency response of one input output combination and $\mathbf{H}$ the corresponding data set of the fitted system.

A. Single-Variable Dependencies

Tab. II shows a summary of validation results for the single-variable dependencies. All median NRMSEs are higher than 98 %, which indicates that the model is a good approximation for the majority of input-output combinations at the analyzed operating points. For many of the input dependencies, the minimum NRMSE is higher than 99 %, which means that even in the worst case of the analyzed operating points the fit approximates the analytical model with high accuracy.

B. Pairwise Combined Variable Dependencies

Fig. 5 shows the validation results for the combined sweep dependencies. As there are 42 individual transfer functions at each operating point, a large number of transfer functions, and consequently, error measurements are generated. Therefore, the NRMSE values for all combinations are summarized in a box plot showing the medians, 25$^{\mathrm{th}}$ and 75$^{\mathrm{th}}$ quartiles, and the extremes (excluding outliers). As expected, the fits have increased error compared to the individual input sweeps in both cases. However, most of the fit percentages remain quite high, i.e. the median fits are all above 98 % and 94 % for the VSM and VDC system, respectively.

The input combinations with the worst fitting results can be directly correlated to the single-variable sweep fits. For example, the lowest mean individual fits in the VSM system are ω_g, ω^*, and p^*, in that respective order. It can be seen that the worst three combined input sweep fits are those that contain a combination of these inputs. The next worst fits contain only one of these three inputs.

Fig. 6 shows the worst single fit operating point for an input and output in the VSM system, at $\omega^* = 0.971, v_{gd} = 0.9$. Note that this fit is not shown in the boxplot as outliers are not shown. This case is quite representative of the the worst fits for the other combinations. While sweeping along ω^*, the frequency responses seem to be mismatched in operating point, meaning that the responses would match more closely with a shifted operating point for the superposition model. This occurs consistently for sweeps including ω^* at $\omega^* =$

TABLE II: Results for Individual Input Dependencies

Model	Input	NRMSE in %		Model	Input	NRMSE in %	
		min.	median			min.	median
VSM	p^*	99.49	99.94	Vdc	$i_{\mathrm{l,q}}*$	75.67	99.60
VSM	q^*	99.99	100.0	Vdc	v_{g}	99.85	99.99
VSM	v_{g}	99.94	100.0	Vdc	ω_{g}	100.0	100.0
VSM	v^*	99.91	99.99	Vdc	$i_{\mathrm{dc,s}}$	75.41	99.24
VSM	ω_{g}	96.81	99.63	Vdc	v^*_{dc}	99.43	99.91
VSM	ω^*	94.92	99.66				

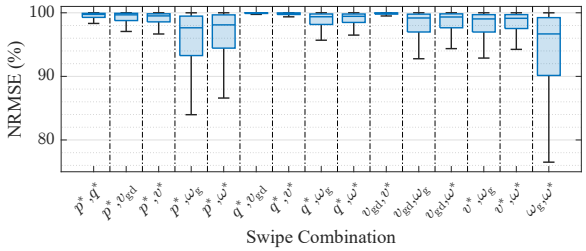

(a) VSM

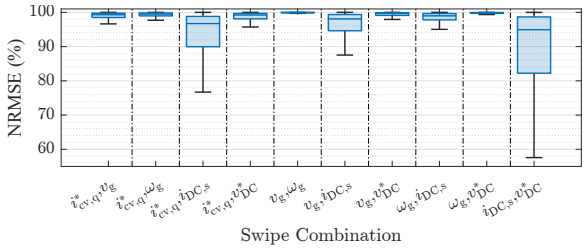

(b) Vdc

Fig. 5: Boxplots of NRMSE for combined sweeps

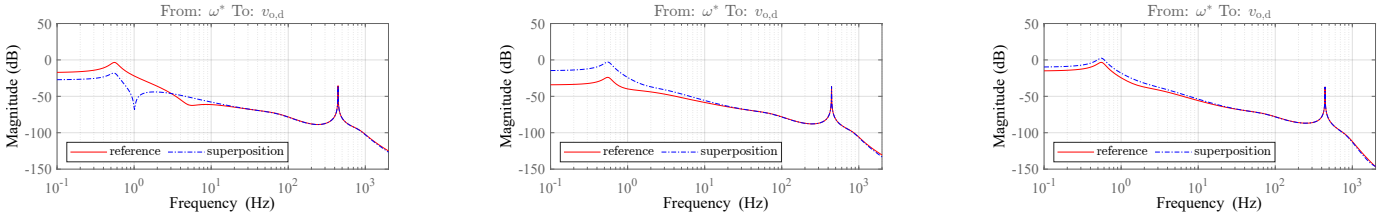

(a) $\omega^* = 0.968, v_{gd} = 0.9$ (b) $\omega^* = 0.971, v_{gd} = 0.9$ (c) $\omega^* = 0.974, v_{gd} = 0.9$

Fig. 6: Worst case combined sweep

0.971, where the frequency response changes rapidly from operating point to operating point, and similar phenomena can be observed for other inputs. This may indicate that a different method of examining the error is needed to account for mismatch in the operating point.

The fitting of the VDC system results in generally worse fit quality than the VSM system. This is expected, due to the difficulty in fitting the eigenvalues as discussed in Section IV-B. Therefore, the behavior of the poles clearly must be examined in the fitting process. However, if the input range is limited such that no bifurcation of the poles is included, a fairly good fit of the system can be achieved.

VI. Conclusion

This work presents an approach for representing the operating point dependency in small-signal state-space models of power electronic converters. The proposed approach is based on expressing the state-space matrices in modal form and fitting each matrix element with a polynomial expression of the input variables. The fitting functions are obtained as a superposition of polynomial expressions for the individual variables. This allows the approximation of the linearized state-space models for all operating conditions within a defined range of input variables from a unified input-dependent state-space representation. The primary intended application area is for representing the operating-point dependent non-linearity of system models obtained by black-box identification methods.

The presented results, obtained with two different cases of control for a grid-connected power converter, indicate that the methodology can provide a high level of fitting with quadratic expressions for the matrix elements. The modal form proved to be valuable to maintain a consistent structure of the matrices over the operating point range. However, the method shows limitations for cases when two real poles bifurcate into a couple of complex conjugated poles, or vice versa. In the studied case with a dc voltage controller, this proved to limit the range of applicability of the proposed polynomial representation of the matrix elements. One possible solution is to repeat the process by splitting the overall range of operating conditions into smaller intervals without internal bifurcations. However, this results in a more time consuming and tedious process for obtaining a set of applicable models, and implies that different models must be used in the different intervals. Evaluation of other alternative representations of an identified state-space model that could avoid this issue is left for further research.

References

[1] P. S. Kundur and O. P. Malik, *Power system stability and control*. McGraw-Hill Education, 2022.

[2] N. Hatziargyriou, J. Milanovic, C. Rahmann, V. Ajjarapu, C. Canizares, I. Erlich, D. Hill, I. Hiskens, I. Kamwa, B. Pal, P. Pourbeik, J. Sanchez-Gasca, A. Stankovic, T. Van Cutsem, V. Vittal, and C. Vournas, "Definition and classification of power system stability – revisited i& extended," *IEEE Trans. on Power Syst.*, vol. 36, no. 4, pp. 3271–3281, 2021.

[3] S. D'Arco, J. Beerten, and J. A. Suul, "Eigenvalue-based analysis of small-signal dynamics and stability in dc grids," in *Modeling, Operation, and Analysis of DC Grids*. Elsevier, 2021, pp. 69–128.

[4] M. Cheah-Mane, A. Egea-Alvarez, E. Prieto-Araujo, H. Mehrjerdi, O. Gomis-Bellmunt, and L. Xu, "Modeling and analysis approaches for small-signal stability assessment of power-electronic-dominated systems," *Wiley Interdisciplinary Reviews: Energy and Environment*, vol. 12, no. 1, p. e453, 2023.

[5] A. Rygg and M. Molinas, "Apparent impedance analysis: A small-signal method for stability analysis of power electronic-based systems," *IEEE J. Emerg. Sel. Topics Power Electron.*, vol. 5, no. 4, pp. 1474–1486, 2017.

[6] M. K. Bakhshizadeh, C. Yoon, J. Hjerrild, C. L. Bak, Ł. H. Kocewiak, F. Blaabjerg, and B. Hesselbæk, "The application of vector fitting to eigenvalue-based harmonic stability analysis," *IEEE J. Emerg. Sel. Topics Power Electron.*, vol. 5, no. 4, pp. 1487–1498, 2017.

[7] D. Deschrijver, T. Dhaene, and D. De Zutter, "Robust Parametric Macromodeling Using Multivariate Orthonormal Vector Fitting," *IEEE Trans. Microwave Theory and Techniques*, vol. 56, no. 7, pp. 1661–1667, Jul. 2008.

[8] P. Triverio, S. Grivet-Talocia, and M. S. Nakhla, "A Parameterized Macromodeling Strategy With Uniform Stability Test," *IEEE Transactions on Advanced Packaging*, vol. 32, no. 1, pp. 205–215, Feb. 2009.

[9] S. B. Olivadese, G. Signorini, S. Grivet-Talocia, and P. Brenner, "Parameterized and DC-Compliant Small-Signal Macromodels of RF Circuit Blocks," *IEEE Trans. on Components, Packaging and Manufacturing Technol.*, vol. 5, no. 4, pp. 508–522, Apr. 2015.

[10] S. Grivet-Talocia and R. Trinchero, "Behavioral, Parameterized, and Broadband Modeling of Wired Interconnects With Internal Discontinuities," *IEEE Trans. Electromag. Compat.*, vol. 60, no. 1, pp. 77–85, Feb. 2018.

[11] T. Bradde, P. Toledo, M. De Stefano, A. Zanco, S. Grivet-Talocia, and P. Crovetti, "Enabling fast power integrity transient analysis through parameterized small-signal macromodels," in *2019 Int. Symp. Electromag. Compat. - EMC EUROPE*, Sep. 2019, pp. 759–764, iSSN: 2325-0364.

[12] L. Reis, "Model Identification of Power Electronic Systems for Interaction Studies and Small-Signal Analysis," Master's thesis, University of Kaiserslautern-Landau, Germany, April 2023. [Online]. Available: https://kluedo.ub.rptu.de/frontdoor/index/index/docId/7310

[13] O. Mo, S. D'Arco, and J. A. Suul, "Evaluation of Virtual Synchronous Machines With Dynamic or Quasi-Stationary Machine Models," *IEEE Trans. Ind. Electron.*, vol. 64, no. 7, pp. 5952–5962, Jul. 2017.

[14] S. D'Arco, J. A. Suul, and J. Beerten, "Configuration and Model Order Selection of Frequency-Dependent Models for Representing DC Cables in Small-Signal Eigenvalue Analysis of HVDC Transmission Systems," *IEEE J. Emerg. and Sel. Topics Power Electron.*, vol. 9, no. 2, pp. 2410–2426, Apr. 2021.